The Non-Ideality in Thymol+Menthol Type V Deep Eutectic Solvents

Journal:	*The Journal of Physical Chemistry Letters*
Manuscript ID	Draft
Manuscript Type:	Letter
Date Submitted by the Author:	n/a
Complete List of Authors:	Schaeffer, Nicolas; Universidade de Aveiro CICECO, Chemistry Abranches, Dinis O.; University of Aveiro, Silva, Liliana; Universidade de Aveiro CICECO, chemistry Martins, Mónia; Universidade de Aveiro, Chemistry Carvalho, Pedro; Universidade de Aveiro Departamento de Quimica, Departamento de Química Russina, Olga; Università di Roma, 'La Sapienza', Dipartimento di Chimica Triolo, Alessandro; Consiglio Nazionale delle Ricerche, Istituto di Struttura della Materia Paccou, Laurent; Unite Materiaux et Transformations Guinet, Yannick; Unite Materiaux et Transformations Hedoux, Alain; University of Lille Faculty of Science and Technology, UMET Coutinho, Joao; Universidade de Aveiro, Química

The Non-Ideality in Thymol+Menthol Type V Deep Eutectic Solvents

Nicolas Schaeffer,[a] Dinis O. Abranches,[a] Liliana P. Silva,[a] Mónia A.R. Martins,[a] Pedro J. Carvalho,[a] Olga Russina,[b,c] Alessandro Triolo,[b] Laurent Paccou,[d] Yannick Guinet,[d] Alain Hedoux,[d] João A.P. Coutinho[a*]

[a] CICECO –Aveiro Institute of Materials, Department of Chemistry, University of Aveiro, 3810-1933 -Aveiro, Portugal

[b] Laboratorio Liquidi Ionici, Istituto Struttura della Materia, Consiglio Nazionale delle Ricerche, (ISM-CNR), Rome, Italy

[c] Department of Chemistry, University of Rome Sapienza, Rome, Italy

[d] Univ. Lille, CNRS, INRAE, Centrale Lille, UMR 8207 - UMET - Unité Matériaux et Transformations, F-59000 Lille, France

* Corresponding author: jcoutinho@ua.pt

ABSTRACT

The non-ionic Type V DES Thymol+Menthol is experimentally and computationally studied aiming to clarify the relation between its liquid phase structure and its thermodynamic non-ideality. ^{1}H-NMR, Raman and X-ray scattering analysis of the Thymol+Menthol system, supported by molecular dynamics simulations, show complex intermolecular interactions dominated by sterically hindered H-bonding clusters. For temperatures greater than or equal to room temperature, a quasi-linear evolution of the eutectic system properties between the pure compounds is observed, suggesting the absence of a magic stochiometric composition in the eutectic solvent. However, temperature dependent Raman spectroscopy indicates a notable increase in thymol-menthol H-bonding as temperatures approach the eutectic point. This study shows that non-ionic Type V DES present an important temperature-dependent non-ideality originating from the change in the intermolecular H-bonding with temperature. These findings have significant implications for the design and growing application of Type V DES.

MANUSCRIPT

Recently, a new class of non-ionic deep eutectic solvents (DES), labelled as Type V DES, in contrast to the ionic nature of Type I to IV, was identified.[1–3] Type V DES exhibit strong negative deviations from ideality, defined by the variation in the activity coefficient of the system, resulting in a significant depression of the melting point that in the case of the 1:1 Thymol+Menthol mixture is 60 K below that predicted for an ideal mixture.[1,4] These non-ionic DES, which are often hydrophobic, appear as promising media for the solvent extraction of organic and metallic compounds presenting low viscosity whilst incorporating bio-derived constituents.[4–8] Despite their potential, characterisation of the condensed phase of Type V DES beyond simple pairwise interaction of the hydrogen bond donor (HBD) and acceptor (HBA) is still scarce. In this work, the molecular interactions of the prototypical Type V DES Thymol+Menthol are experimentally and computationally studied aiming to understand its liquid phase structure and its relation to non-ideality. The system Thymol+Menthol is particularly interesting as, although both substances are structurally similar (structures shown in **Figure 1**), both compounds present severe negative deviations to thermodynamic ideality when mixed. Hydrogen bonding (H-bonding) in the mixture is followed by ^{1}H-NMR and Raman spectroscopy as a function of eutectic composition as well as temperature. Additionally, the intermediate range order in the liquid phase structuring of the 1:1 Thymol+Menthol is probed by X-ray scattering. The experimental results are further complemented by molecular dynamic (MD) simulations.

^{1}H-NMR spectra of the Thymol+Menthol liquid phase covering the full composition range is presented in **Figure S1**, with the change in chemical shift of selected protons ($\Delta\delta_H$) highlighted in **Figure 1**. Gradual addition of thymol to menthol results in a respective upshift and downshift of their proton chemical shifts relative to the pure compounds. The rise in $\Delta\delta_H$ of thymol in presence of menthol is indicative of thymol protons in a less shielded environment and their overall greater acidity with increasing menthol molar fraction ($x_{Menthol}$), with the opposite being observed for menthol at increasing thymol molar fractions (x_{Thymol}). The magnitude of $\Delta\delta_H$ is highly dependent on the proton position in each molecule with the hydroxyl proton presenting the largest $\Delta\delta_H$ values. An increase in H-bonding removes electron density from the local vicinity of the nucleus, making the nuclei less shielded with respect to the applied magnetic field. This is consistent with the formation of an intermolecular H-bonded network in the DES liquid phase driven by the greater acidity of the phenolic hydrogen, making thymol an excellent HBD.[1,9] The preferential nature of the thymol(OH)···(OH)menthol H-bond is evidenced by the

$\Delta\delta_H$= 1.73 ppm of the thymol hydroxide for x_{Thymol}= 0.5 and appears as the main driving force for the system non-ideality. However, the observed $\Delta\delta_H$ is lower than the $\Delta\delta_H$= 4.10 ppm in the equimolar Thymol+Trioctylphosphine oxide mixture due to the greater Lewis basicity of the phosphine oxide bond compared to alcohols.[7] The downshift in the menthol hydroxide $\Delta\delta_H$ relative to its pure state with increasing x_{Thymol} is attributed to the decrease in inter menthol H-bonding due to competing presence of the more acidic proton of thymol as HBD. Interestingly, the magnitude of $\Delta\delta_H$ for similarly positioned protons group in thymol and menthol excluding the hydroxyl group do not follow identical trends, **Figure 1**. The nearest proton to the hydroxyl group in thymol exhibits the second greatest upshift but presents the smallest shift in menthol. Conversely, the thymol ring hydrogen in the para-position from the hydroxyl group displays the smallest $\Delta\delta_H$, in accordance with resonance effects in the thymol aromatic ring, but the second largest in menthol. This suggests that relative to the interactions in their pure liquid state, H-bonding is reinforced for thymol molecules in the Thymol+Menthol DES whilst additional dispersive interactions combined with H-bonding stabilise menthol molecules.

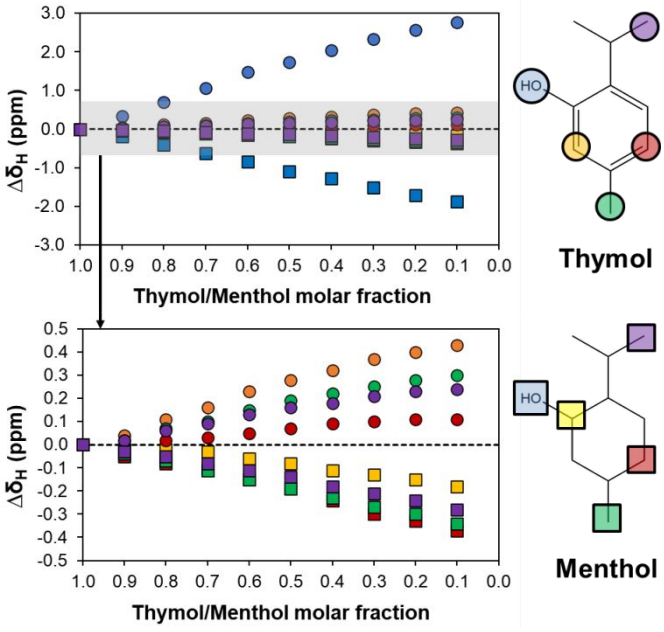

Figure 1. Change in ^{1}H-NMR chemical shift of select highlighted protons ($\Delta\delta_H$) of thymol (circles) and menthol (squares) in the Thymol+Menthol eutectic as a function of composition at T = 328 K. A molar fraction of 1.0 corresponds to the pure individual component; all compositions are in the liquid state.

Reduction of the Thymol+Menthol system to simple binary interactions, thymol-menthol *vs* the pure compounds with themselves, provides only a partial picture considering H-bonded liquids can assemble into extended H-bonding networks and oligomers.[10] Small angle X-ray scattering (SAXS) analysis of the liquid 1:1 Thymol+Menthol DES (T = 293 K) in **Figure 2** clearly shows the presence of a prepeak at 6.0 nm^{-1}, corresponding to the distance of 1.05 nm (=$2\pi/6.0$ nm^{-1}), appearing much before the standard peak associated to neighbour alkyl moieties at 12.5 nm^{-1}.[11] Such prepeaks are commonly observed in covalent and ionic glasses or melts[12] and more unexpectedly in certain molecular "fragile" glass-forming liquids including alcohols as well as ionic liquids.[10,13–16] The existence of the prepeak is usually interpreted as evidence of an intermediate-range order (the length is greater than the 1st shell of neighbour molecules) due to the existence of H-bond-induced heterogeneities or clusters. Contrary to H-bonded liquids with reduced packing constraints like glycerol or methanol, steric exclusion between the ring of menthol and/or thymol prevents formation of a continuous H-bond network resulting instead in smaller H-bonded clusters presenting a hydroxyl rich core and a alkyl rich exterior.[13] Changes in the eutectic components can potentially promote additional intermediate range ordering of the liquid phase. For example. small angle neutron scattering (SANS) of the thermodynamically ideal mixture of Menthol+Decanoic acid[3] suggests the presence of weakly interacting micellar-like spherical aggregates.[17]

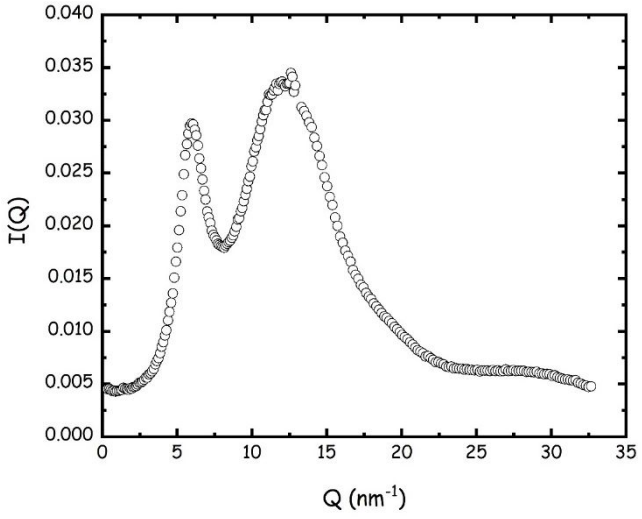

Figure 2. X-ray scattering profile of the liquid 1:1 Thymol+Menthol DES ($T \approx 293$ K).

The H-bonding in the Thymol+Menthol system was further probed at different molar compositions by Raman spectroscopy in the 2600-4000 cm^{-1} region, shown in **Figure 3A**. For increased clarity, the spectra in the OH stretching (ν(OH)) region were deconvoluted into Gaussian-shape components based on the dominant peaks of the pure compounds, with selected examples presented in **Figure 3B**. Due to the difficulty in the unequivocal assignment of spectral distributions to specific H-bonded species in the undiluted eutectic, this was not attempted here. Rather, the Raman ν(OH) spectrum was analysed in terms of different contribution depending on their involvement in the H-bond formation, namely into α, β, γ and δ OHs.[18,19] "Free" hydroxyl groups not involved in hydrogen-bonding, corresponding to α and β OHs, were detected at around 3620 cm^{-1} in the studied system and correspond to the grey band in the deconvoluted spectra in **Figure 3B**.[20] Terminal proton-donating OH bonds, with lone pairs of the O atom not involved in hydrogen bonds (γ OH), only partially contribute to the H-bonded network through dimer formation. The corresponding band is detected at approximately 3540 cm^{-1} and identified by the orange band in the deconvoluted spectra. Finally, proton accepting and donating δ OHs detected at lower wavenumbers are responsible for the formation of intra-chain OH bonds resulting in the formation of H-bonded aggregates (green and blue bands in the deconvoluted spectra).

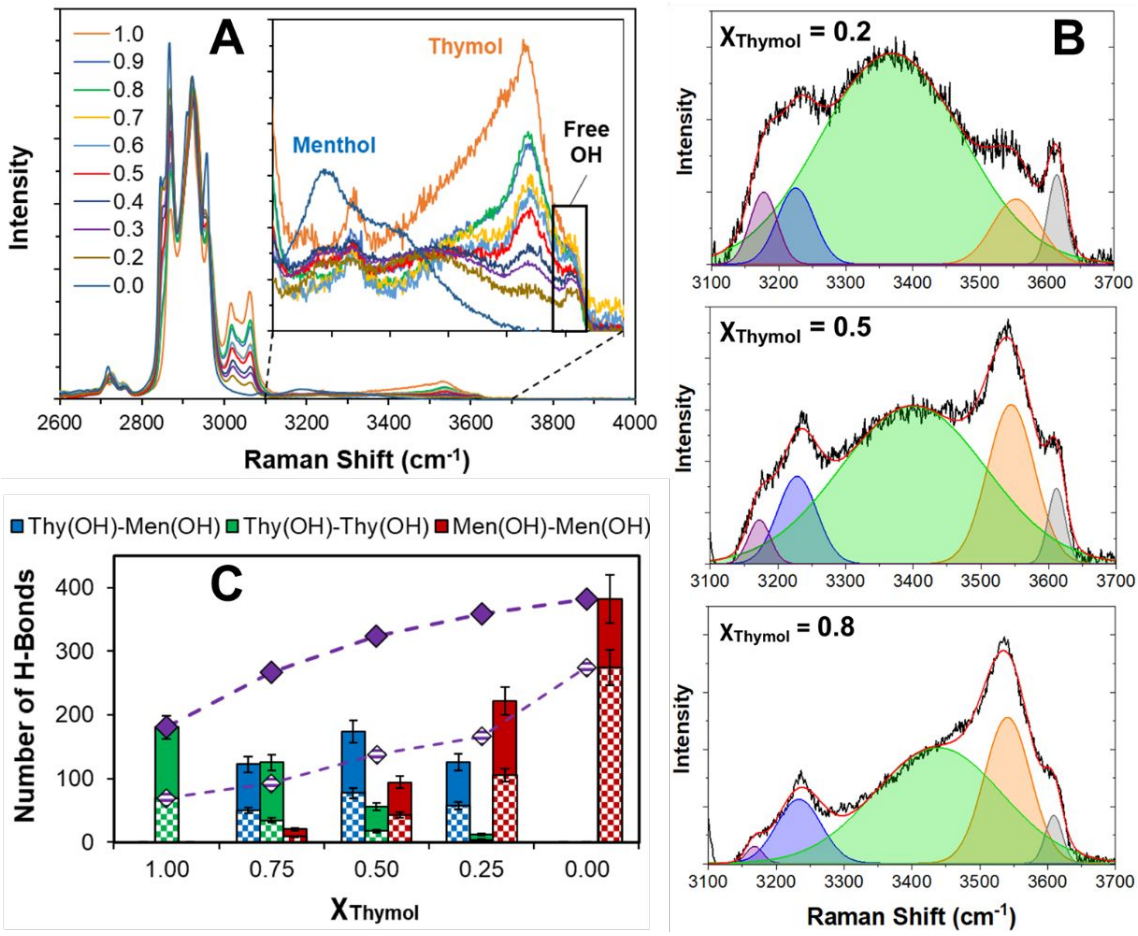

Figure 3. A) Raman spectra of liquid thymol and crystalline menthol and their liquid binary mixtures in the OH stretching region at T = 293 K. B) Deconvoluted Raman spectra for three different χ_{Thymol} concentrations in the range 3100-3700 cm^{-1}, the red line corresponds to the deconvolution fit. C) H-bond distribution in the MD simulations of the Thymol+Menthol system for three different compositions (T= 330 K; 400 molecules). H-bonding analysis[21] was performed with geometric criteria for weak (full bars; r ≤ 0.35 nm, angle ≤ 90°) and medium (pattern bars; r ≤ 0.30 nm, angle ≤ 30°) H-bonds.

The large gap in the melting and crystallization temperature of thymol provides sufficient longevity to the metastable liquid state, allowing to study the full range of composition on the thymol side of the Thymol+Menthol phase diagram at room temperature.[1] The Raman spectra of metastable liquid thymol, i.e. non-crystalline, covers a wide wavenumber range (3200 – 3650 cm^{-1}) but is dominated by the γ OH band at 3530 cm^{-1} confirming thymol as an excellent H-bond donor but poor H-bond receptor. This in turn restricts the formation of larger hydrogen bonded oligomers and is consistent with the limited self-association of the structurally similar

phenol in aprotic organic solvents.[22] Additionally, the free OH band is clearly observable at 3620 cm^{-1}. Compared to thymol, menthol as a classical alcohol can act both as a H-bond donor and acceptor in equal measure, promoting a more efficient H-bonding.[10] Classical MD simulations of the pure thymol and menthol condensed phase at 330 K confirm the lesser number and weaker average energy of H-bonds in thymol (ΔG=10.5 $kJ.mol^{-1}$) compared to in liquid menthol (ΔG=21.4 $kJ.mol^{-1}$), **Figure S2** and **Figure 3C**. Addition of thymol in menthol induces the breaking of strong H-bond molecular associations, and vice versa for addition of menthol in thymol, with observation of persistent free OH groups not involved in molecular associations even at low thymol molar fractions (x_{Thymol}=0.2 in **Figure 3B**). Results indicate that the Thymol+Menthol DES structural organisation involves three types of molecular associations, menthol-menthol via stronger H-bonds, thymol-thymol via weaker H-bonds and thymol-menthol via mixed strength bonding, characterized by the δ OH stretching band (green) around 3400 cm^{-1}. Decreasing x_{Thymol} in the eutectic mixture results in the linear decrease in the deconvoluted area of the γ OH band (orange) of thymol but in the increase of the δ OH stretching band (green), **Figure S3**.

Figure S4 in the ESI shows that MD-derived x-ray scattering pattern[23] nicely accounts for the experimental structural features shown in **Figure 2**, thus providing support to the ability of the chosen potential to reproduce structural features of the Thymol:Menthol mixture. Radial distribution function (RDF) analysis and the derived coordination number (CN) obtained from MD simulations of the Thymol+Menthol system for three molar ratios (x_{Thymol} of 0.25, 0.50 and 0.75) indicate the Thymol(H)···(O)Menthol H-bond as the predominant short range (≤ 0.2 nm) H-bond interaction followed by inter-menthol H-bonding for all compositions, **Figure S5**. Extending the geometry criteria for H-bond to include an HBD-HBA distance and a D–H–A angle characteristic of weak (r ≤ 0.35 nm, angle ≤ 90°) and medium (r ≤ 0.30 nm, angle ≤ 30°) H-bond[24] reveals a variable H-bond distribution between thymol-menthol, thymol-thymol and menthol-menthol dependent on the eutectic composition, **Figure 3C.** Increasing x_{Thymol} results in a decrease in the total number of H-bond of the system driven by the reduction in menthol-menthol interaction, the dominant H-bond at lower x_{Thymol}, due to the competing nature of the stronger thymol-menthol hydrogen bond as also shown in **Figure 1**. At higher x_{Thymol} composition, the eutectic solvent is characterized by thymol-menthol H-bonding even in the presence of excess thymol molecules. The number of thymol-menthol H-bonds presents a maximum for equimolar composition. The H-bond criteria does not appear to influence the overall H-bond distribution trend in the studied systems, **Figure 3C**. However, a sharper

decrease in menthol-menthol H-bond numbers is observed for stronger H-bonds ($r \leq 0.30$ nm, angle $\leq 30°$) as thymol (x_{Thymol}=0.25) is added to pure menthol, in line with the Raman spectra in **Figure 3** indicating weaker H-bonding associations with increasing thymol content. 3D spatial density function (SDF) plot of the 1:1 Thymol+Menthol system projecting the most probable configurations of the various system components is presented in **Figure S6**. SDF plot clearly shows the presence of the menthol hydroxide group in both HBD and HBA acceptor configurations. In contrast, the spatial localisation of the thymol hydroxide group surface around the reference confirms thymol's primary contribution as an HBD. Furthermore, whilst menthol molecules adopt a "head-on" arrangement to maximise H-bonding, the thymol surface surrounding the menthol alkyl regions suggests additional dispersive interactions in addition to H-bonding. This is in accordance with the important $\Delta\delta_H$ downshift in the menthol ring proton with increasing x_{Thymol} in **Figure 1** as well as the reported perpendicular T shaped organisation of aromatic compounds with pi-pi interactions.[25]

It is well known that temperature exerts a strong influence on H-bonded systems, with the extent of H-bonding decreasing with temperature increase.[18,26,27] The temperature dependence of the Raman ν(OH) spectrum for Thymol+Menthol at a fixed composition (x_{Thymol}=0.5) was followed from room temperature to just above its glass transition temperature of ~210 K.[1] This composition was selected as it presents the largest liquidus regime with temperature, permitting the study for a wider temperature range. The raw Raman spectra are available in **Figure S7** and the deconvoluted spectra are presented in **Figure 4**. It is clearly observed that the contribution of the lower energy α/β and γ ν(OH) bands decrease for lower temperatures while the higher energy δ ν(OH) bands increase, **Figure S8**. Most notably, the free hydroxyl band of thymol fully disappears at 213 K, indicating the formation of strong intermolecular H-bonding association at the expense of weak H-bonding associations and free OH groups with decreasing temperature. **Figure 4** emphasises the important temperature dependency of Type V eutectics, affecting both the total number of H-bonds in the mixture as well as their strength. This is further confirmed by MD simulations of the liquid Thymol+Menthol system for x_{Thymol}=0.5 at different temperatures from 233 K to 453 K, **Figure S9**. A decrease in the number of H-bonds in the system is observed as well as shift in the H-bonded population from higher ordered oligomers to monomers and dimers with temperature increase.

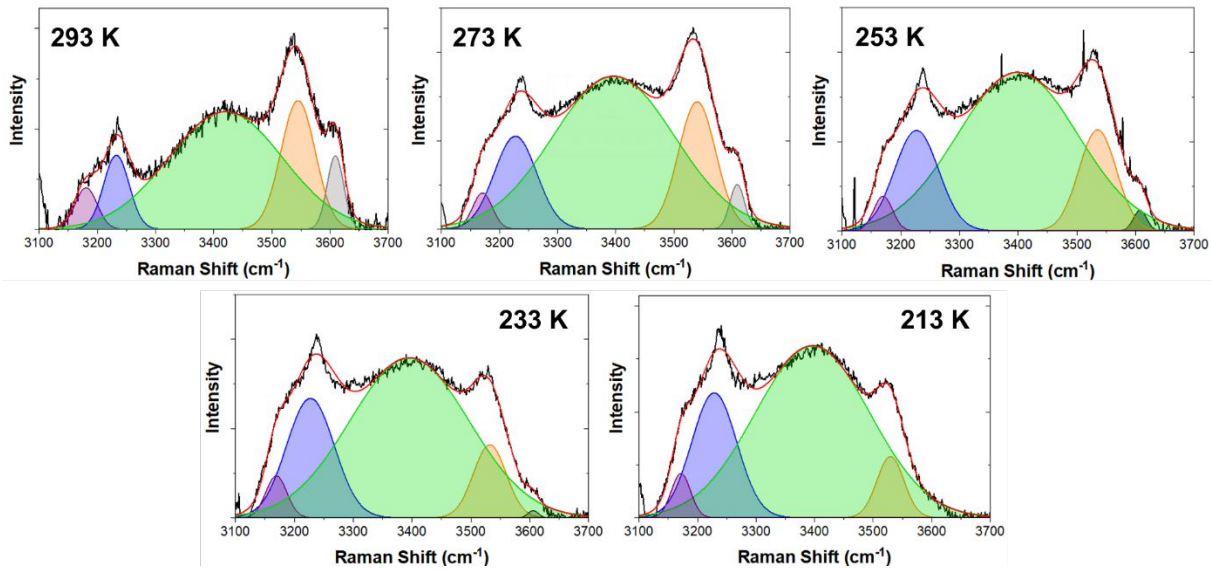

Figure 4. Deconvoluted Raman spectra in the OH stretching region of the liquid Thymol+Menthol eutectic as a function of temperature for a fixed composition (x_{Thymol} =0.5). The red line corresponds to the deconvolution fit; the untreated Raman spectra are available in **Figure S7**.

The Thymol+Menthol system presents complex intermolecular interactions dominated by sterically hindered H-bonding clusters with additional dipolar and van der Waals contribution. Results in **Figure 1** and **3** obtained at room temperature or greater indicate the quasi-linear evolution of the eutectic system properties between the pure compounds. This suggests the absence of a magic stochiometric composition in the eutectic solvent,[28] although small differences in the dominant H-bond interaction with composition (**Figure 3C**), namely the thymol-menthol H-bond, are observed. Rather, **Figure 4** shows a notable increase in H-bonding as temperatures approach the eutectic solid-liquid equilibrium (SLE) conditions driven by the greater inclusion of thymol in H-bonded clusters. It is therefore proposed that the non-ionic Type V DES present a significant temperature-dependent non-ideality originating from the change in the intermolecular H-bonding with temperature. To validate this hypothesis, the isobaric vapour liquid equilibrium (VLE) of Thymol+Menthol at p=500 mbar was estimated using the conductor like screening model for real solvent model (COSMO-RS)[29,30] due to its accurate description of the Thymol+Menthol system non-ideality **(Figure 5A)**.[1] The estimated VLE is in good agreement with the experimentally determined ebullition point of the mixture at p=500 mbar (**Figure 5A**), validating the use of COSMO-RS as a predictive model for the studied system. The COSMO-RS derived activity coefficients are compared with those

obtained from the SLE (**Figure 5B**), thereby permitting the determination of the upper and lower limit of the Thymol+Menthol liquid phase non-ideality with temperature. An activity coefficient of unity indicates a thermodynamically ideal system. **Figure 5B** confirms the drastic reduction in the non-ideality of the system with temperature increase. The eutectic system is strongly non-ideal near the SLE but quasi-ideal at the VLE, with the activity coefficient of thymol at x_{Thymol} =0.5 varying from below 0.3 at 223 K to approximately 0.9 at 463 K. COSMO-RS prediction of the isothermal activity coefficient for temperatures from 233 K to 373 K is shown in **Figure S10** and indicates a systematic change with temperature in line with the shift in the ν(OH) profile of the eutectic in **Figure 4.**

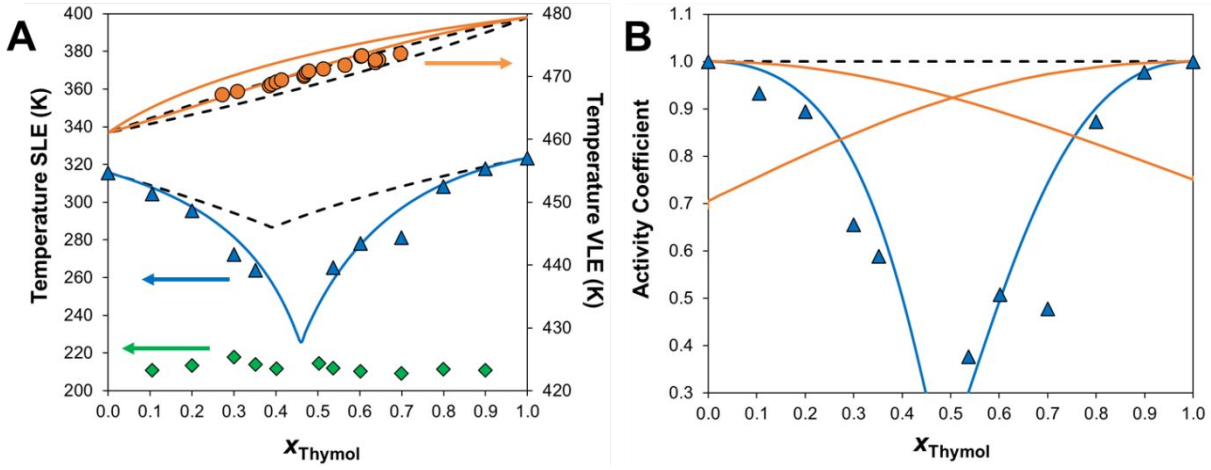

Figure 5. A) Experimental SLE[1] (blue) and isobaric VLE (orange, p= 500 mbar) phase diagram and B) derived activity coefficients for the binary Thymol+Menthol system. The predictions by the ideal liquid or vapour phase model (dashed line) and by COSMO-RS (full line) are included. Glass transition temperatures are shown (♦).

To summarise, Thymol+Menthol are complex H-bonded solutions presenting a strong thermodynamic non-ideality primarily conferred by the dominant intermolecular H-bond between the DES component relative to their self-interaction. Furthermore, the extent of non-ideality is defined by the temperature dependency of H-bonding aggregation in the mixture, this phenomenon being reinforced with decreasing temperature. For experimental temperatures sufficiently high, moderate to negligible deviations from ideality are observed. Most importantly, the presented findings have significant implications for design and application of Type V DES, allowing the latter to be considered as quasi-ideal for sufficiently high

temperatures and permitting a first approximation of the eutectic properties through adequate mixing rules of the pure component properties. COSMO-RS appears as a promising tool for the fast screening of Type V eutectics. Although only the Thymol+Menthol was studied herein, it is expected that the obtained conclusions are transferable to other Type V non-ionic deep eutectic systems. Further work is anticipated to extend this for systems composed of strong HBD (e.g. thymol) with HBA presenting no H-bonding capabilities (e.g. phosphine oxides, sulfoxides or ketones) as their H-bonded network could persist for a wider temperature range due to the poor self-association of each component.

ACKNOWLEDGMENTS

This work was developed within the scope of the project CICECO-Aveiro Institute of Materials, UIDB/50011/2020 & UIDP/50011/2020, financed by national funds through the Foundation for Science and Technology/MCTES. The NMR spectrometers are part of the National NMR Network (PTNMR) and are partially supported by Infrastructure Project Nº 022161 (co-financed by FEDER through COMPETE 2020, POCI and PORL and FCT through PIDDAC). L.P.S. acknowledges FCT for her PhD grant (SFRH/BD/135976/2018). Access to the SAXS-Lab at the University of Rome Sapienza and kind support from Dr. A. Del Giudice are acknowledged. This work has been partially supported by a University of Rome Sapienza grant (RG11715C7CC660BE).

REFERENCES

(1) Abranches, D. O.; Martins, M. A. R.; Silva, L. P.; Schaeffer, N.; Pinho, S. P.; Coutinho, J. A. P. Phenolic Hydrogen Bond Donors in the Formation of Non-Ionic Deep Eutectic Solvents: The Quest for Type V DES. *Chem. Commun.* **2019**, *55* (69), 10253–10256. https://doi.org/10.1039/c9cc04846d.

(2) Smith, E. L.; Abbott, A. P.; Ryder, K. S. Deep Eutectic Solvents (DESs) and Their Applications. *Chemical Reviews*. American Chemical Society November 12, 2014, pp 11060–11082. https://doi.org/10.1021/cr300162p.

(3) Abranches, D. O.; Martins, R. O.; Silva, L. P.; Martins, M. A. R.; Pinho, S. P.; Coutinho, J. A. P. Liquefying Compounds by Forming Deep Eutectic Solvents: A Case Study for

Organic Acids and Alcohols. *J. Phys. Chem. B* **2020**, *124* (20), 4174–4184. https://doi.org/10.1021/acs.jpcb.0c02386.

(4) Martins, M. A. R.; Silva, L. P.; Schaeffer, N.; Abranches, D. O.; Maximo, G. J.; Pinho, S. P.; Coutinho, J. A. P. Greener Terpene-Terpene Eutectic Mixtures as Hydrophobic Solvents. *ACS Sustain. Chem. Eng.* **2019**, *7* (20), 17414–17423. https://doi.org/10.1021/acssuschemeng.9b04614.

(5) Kaul, M. J.; Qadah, D.; Mandella, V.; Dietz, M. L. Systematic Evaluation of Hydrophobic Deep-Melting Eutectics as Alternative Solvents for the Extraction of Organic Solutes from Aqueous Solution. *RSC Adv.* **2019**, *9* (28), 15798–15804. https://doi.org/10.1039/c9ra01596e.

(6) Křížek, T.; Bursová, M.; Horsley, R.; Kuchař, M.; Tůma, P.; Čabala, R.; Hložek, T. Menthol-Based Hydrophobic Deep Eutectic Solvents: Towards Greener and Efficient Extraction of Phytocannabinoids. *J. Clean. Prod.* **2018**, *193*, 391–396. https://doi.org/10.1016/j.jclepro.2018.05.080.

(7) Schaeffer, N.; Conceiçaõ, J. H. F.; Martins, M. A. R.; Neves, M. C.; Pérez-Sánchez, G.; Gomes, J. R. B.; Papaiconomou, N.; Coutinho, J. A. P. Non-Ionic Hydrophobic Eutectics-Versatile Solvents for Tailored Metal Separation and Valorisation. *Green Chem.* **2020**, *22* (9), 2810–2820. https://doi.org/10.1039/d0gc00793e.

(8) Silva, N. H. C. S.; Morais, E. S.; Freire, C. S. R.; Freire, M. G.; Silvestre, A. J. D. Extraction of High Value Triterpenic Acids from Eucalyptus Globulus Biomass Using Hydrophobic Deep Eutectic Solvents. *Molecules* **2020**, *25* (1), 210. https://doi.org/10.3390/molecules25010210.

(9) Graton, J.; Besseau, F.; Brossard, A. M.; Charpentier, E.; Deroche, A.; Le Questel, J. Y. Hydrogen-Bond Acidity of OH Groups in Various Molecular Environments (Phenols, Alcohols, Steroid Derivatives, and Amino Acids Structures): Experimental Measurements and Density Functional Theory Calculations. *J. Phys. Chem. A* **2013**, *117* (49), 13184–13193. https://doi.org/10.1021/jp410027h.

(10) Böhmer, R.; Gainaru, C.; Richert, R. Structure and Dynamics of Monohydroxy Alcohols-Milestones Towards Their Microscopic Understanding, 100 Years After Debye. *Physics Reports*. Elsevier B.V. 2014, pp 125–195. https://doi.org/10.1016/j.physrep.2014.07.005.

(11) Yoshida, K.; Fukuyama, N.; Yamaguchi, T.; Hosokawa, S.; Uchiyama, H.; Tsutsui, S.; Baron, A. Q. R. Inelastic X-Ray Scattering on Liquid Benzene Analyzed Using a Generalized Langevin Equation. *Chem. Phys. Lett.* **2017**, *680*, 1–5. https://doi.org/10.1016/j.cplett.2017.05.005.

(12) Elliott, S. R. The Origin of the First Sharp Diffraction Peak in the Structure Factor of Covalent Glasses and Liquids. *J. Phys. Condens. Matter* **1992**, *4* (38), 7661–7678. https://doi.org/10.1088/0953-8984/4/38/003.

(13) Morineau, D.; Alba-Simionesco, C.; Bellissent-Funel, M. C.; Lauthié, M. F. Experimental Indication of Structural Heterogeneities in Fragile Hydrogen-Bonded Liquids. *Europhys. Lett.* **1998**, *43* (2), 195–200. https://doi.org/10.1209/epl/i1998-00339-6.

(14) Morineau, D.; Alba-Simionesco, C. Hydrogen-Bond-Induced Clustering in the Fragile Glass-Forming Liquid m-Toluidine: Experiments and Simulations. *J. Chem. Phys.* **1998**, *109* (19), 8494–8503. https://doi.org/10.1063/1.477514.

(15) Tomšič, M.; Jamnik, A.; Fritz-Popovski, G.; Glatter, O.; Vlček, L. Structural Properties of Pure Simple Alcohols from Ethanol, Propanol, Butanol, Pentanol, to Hexanol: Comparing Monte Carlo Simulations with Experimental SAXS Data. *J. Phys. Chem. B* **2007**, *111* (7), 1738–1751. https://doi.org/10.1021/jp066139z.

(16) Russina, O.; Triolo, A.; Gontrani, L.; Caminiti, R. Mesoscopic Structural Heterogeneities in Room-Temperature Ionic Liquids. *J. Phys. Chem. Lett.* **2012**, *3* (1), 27–33. https://doi.org/10.1021/jz201349z.

(17) Percevault, L.; Jani, A.; Sohier, T.; Noirez, L.; Paquin, L.; Gauffre, F.; Morineau, D. Do Deep Eutectic Solvents Form Uniform Mixtures Beyond Molecular Microheterogeneities? *J. Phys. Chem. B* **2020**, acs.jpcb.0c06317. https://doi.org/10.1021/acs.jpcb.0c06317.

(18) Paolantoni, M.; Sassi, P.; Morresi, A.; Cataliotti, R. S. Infrared Study of 1-Octanol Liquid Structure. *Chem. Phys.* **2005**, *310* (1–3), 169–178. https://doi.org/10.1016/j.chemphys.2004.10.027.

(19) Paolantoni, M.; Sassi, P.; Morresi, A.; Cataliotti, R. S. Raman Noncoincidence Effect on OH Stretching Profiles in Liquid Alcohols. *J. Raman Spectrosc.* **2006**, *37* (4), 528–

537. https://doi.org/10.1002/jrs.1427.

(20) Palombo, F.; Paolantoni, M.; Sassi, P.; Morresi, A.; Cataliotti, R. S. Spectroscopic Studies of the "Free" OH Stretching Bands in Liquid Alcohols. *J. Mol. Liq.* **2006**, *125* (2–3), 139–146. https://doi.org/10.1016/j.molliq.2005.11.006.

(21) Van Der Spoel, D.; Van Maaren, P. J.; Larsson, P.; Tîmneanu, N. Thermodynamics of Hydrogen Bonding in Hydrophilic and Hydrophobic Media. *J. Phys. Chem. B* **2006**, *110* (9), 4393–4398. https://doi.org/10.1021/jp0572535.

(22) Woolley, E. M.; Hepler, L. G. Molecular Association of Hydrogen Bonding Solutes. Phenol in Cyclohexane and Benzene. *J. Phys. Chem.* **1972**, *76* (21), 3058–3064. https://doi.org/10.1021/j100665a026.

(23) Hollóczki, O.; Macchiagodena, M.; Weber, H.; Thomas, M.; Brehm, M.; Stark, A.; Russina, O.; Triolo, A.; Kirchner, B. Triphilic Ionic-Liquid Mixtures: Fluorinated and Non-Fluorinated Aprotic Ionic-Liquid Mixtures. *ChemPhysChem* **2015**, *16* (15), 3325–3333. https://doi.org/10.1002/cphc.201500473.

(24) Jeffrey, G. A. *An Introduction to Hydrogen Bonding*; Oxford University Press: New York, 1997.

(25) Headen, T. F.; Howard, C. A.; Skipper, N. T.; Wilkinson, M. A.; Bowron, D. T.; Soper, A. K. Structure of π-π Interactions in Aromatic Liquids. *J. Am. Chem. Soc.* **2010**, *132* (16), 5735–5742. https://doi.org/10.1021/ja909084e.

(26) Wallen, S. L.; Palmer, B. J.; Garrett, B. C.; Yonker, C. R. Density and Temperature Effects on the Hydrogen Bond Structure of Liquid Methanol. *J. Phys. Chem.* **1996**, *100* (10), 3959–3964. https://doi.org/10.1021/jp9524082.

(27) Dougherty, R. C. Temperature and Pressure Dependence of Hydrogen Bond Strength: A Perturbation Molecular Orbital Approach. *J. Chem. Phys.* **1998**, *109* (17), 7372–7378. https://doi.org/10.1063/1.477343.

(28) Alizadeh, V.; Malberg, F.; Pádua, A. A. H.; Kirchner, B. Are There Magic Compositions in Deep Eutectic Solvents? Effects of Composition and Water Content in Choline Chloride/Ethylene Glycol from Ab Initio Molecular Dynamics. *J. Phys. Chem. B* **2020**, *2020*, 7433–7443. https://doi.org/10.1021/acs.jpcb.0c04844.

(29) Klamt, A. Conductor-like Screening Model for Real Solvents: A New Approach to the

Quantitative Calculation of Solvation Phenomena. *J. Phys. Chem.* **1995**, *99* (7), 2224–2235. https://doi.org/10.1021/j100007a062.

(30) Klamt, A.; Jonas, V.; Bürger, T.; Lohrenz, J. C. W. Refinement and Parametrization of COSMO-RS. *J. Phys. Chem. A* **1998**, *102* (26), 5074–5085. https://doi.org/10.1021/jp980017s.

GRAPHICAL ABSTRACT

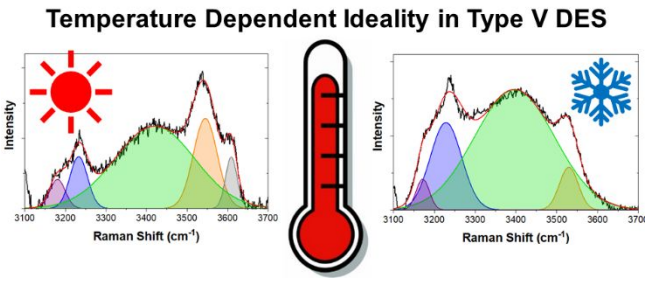

SYNOPSIS

Type V DES present a temperature-dependent non-ideality originating from the change in the intermolecular hydrogen-bonding with temperature.